

## Robust and high barrier thermoplastic starch – PLA blend films using starch-graft-poly (lactic acid) as a compatibilizer

Binh M. Trinh, Debela T. Tadele, Tizazu H. Mekonnen

Department of Chemical Engineering, Institute of Polymer Research, Waterloo Institute of Nanotechnology, University of Waterloo, Waterloo, ON, Canada

Corresponding author: [tmekonnen@uwaterloo.ca](mailto:tmekonnen@uwaterloo.ca)

**Table S1:** Thermal properties of TPS, PLA, and TPS/PLA blends obtained by DSC

Sample film	T <sub>g</sub> (PLA phase) (°C)	T <sub>cc</sub> (°C)	ΔH <sub>cc</sub> (J/g)	T <sub>m</sub> (°C)	ΔH <sub>m</sub> (J/g)	X <sub>c</sub> (%)
TPS	--	--	--	--	--	--
PLA	56.77	115.63	5.49	147.66	15.15	10.3
TPS/PLA	55.31	117.93	7.50	145.02	15.71	8.21
TPS/PLA/1% St-PLA	53.70	108.88	8.33	141.52, 149.71	11.36	3.23
TPS/PLA/2.5% St-PLA	53.78	106.77	10.65	140.14, 149.56	13.16	2.67
TPS/PLA/5% St-PLA	54.81	114.43	18.41	143.86, 150.92	20.16	1.86

**Table S2:** Summary of tensile properties of TPS, PLA, and TPS/PLA blended film

Sample film	Tensile strength (MPa)	Elongation at break (%)	Elastic modulus (MPa)
TPS	2.33±0.16	67.5±1.3	37.85±4.63
TPS/PLA	5.83±0.84	1.65± 0.38	472.82±75.4
TPS/PLA/1% St-PLA	6.51±0.71	3.23±0.45	490.01±90.42
TPS/PLA/2.5% St-PLA	8.52±0.91	3.71±0.42	631.23±101.25
TPS/PLA/5% St-PLA	10.21±2.15	4.25±0.18	783.18±80.3
PLA	46.04±6.89	5.65±2.59	2020 ± 400

**Table S3:** Summary of optical, and barrier properties of TPS, PLA, and TPS/PLA blended film

Sample film	T% (600nm)	Opacity (A600/mm)	WVP x 10 <sup>-13</sup> (kg.m/s.m <sup>2</sup> .Pa)	OP x 10 <sup>-3</sup> (cm <sup>3</sup> .m/m <sup>2</sup> .day.Pa)
TPS	60.31±1.21	0.80±0.05	13.03±2.18	10.82±0.83
TPS/PLA	32.59±0.81	2.32±0.11	5.90±0.99	39.44±1.15
TPS/PLA/1% St-PLA	41.1±0.80	2.15±0.16	7.40±0.80	33.56±3.42
TPS/PLA/2.5% St-PLA	47.45±1.71	1.81±0.18	7.96±0.16	25.36±0.72
TPS/PLA/5% St-PLA	46.31±0.72	1.79±0.12	8.87±0.42	20.13±1.25
PLA	77.83±1.95	0.41±0.04	3.59±0.16	265.01±15.65

### Dynamic mechanical analysis

The thermomechanical properties of non-compatible TPS/PLA and compatible TPS/PLA/St-PLA blends were evaluated, and results are presented in **Fig S1 (a&b)**. The results of storage modulus ( $E'$ ) as a function of temperature shows that the storage modulus at the start increases with increasing concentration of St-PLA compatibilizer added to the blend, indicating that the compatible blends TPS/PLA/St-PLA exhibited improved synergistic behavior between two phases which result in stiffer materials. This observation agrees with the elastic modulus results. It should also be noted that the compatible TPS/PLA/St-PLA sample displayed a more amorphous behaviour as the slope of storage modulus gradually decreases instead of having a rubbery plateau as that presented in the non-compatible blend, which further indicates that the crystalline structure within TPS/PLA gradually diminished as suggested from the analysis in POM and DSC.

As expected from immiscible blends, all the blended samples typically displayed two distinctive glass transition temperature ( $T_g$ ) peaks of TPS and PLA, respectively. The first single tan delta peak was identified at approximately  $-41\text{ }^\circ\text{C}$ , which belong to the  $T_g$  of TPS phase within the TPS/PLA blend. The other delta peak observed in TPS/PLA blends was attributed to the  $T_g$  of PLA polymer phase, which located around  $65\text{ }^\circ\text{C}$ . Moreover, the mobility of polymer chain segments within the blend can also be interpreted from the peak's intensity of tan delta [1,2]. Gradual reduction and broaden intensity were especially noted with increasing concentration of the compatibilized St-PLA included in the formulation, implying higher restriction of segment motions of PLA chains due to the entanglement with TPS chains, which was caused by the partially miscible bridging by the compatibilizer TPS/PLA. Illustration for this phenomenon can be observed in **Fig S1c**. Furthermore, the emergence of a small peak around  $33\text{-}35\text{ }^\circ\text{C}$  was also observed in all compatibilized TPS/PLA/St-PLA samples. This was possibly related to the phase where TPS and PLA are connected and partially miscible, which was indicative of better interfacial miscibility and compatibility between TPS and PLA being bridged together by the ex-situ co-grafted oligomers.

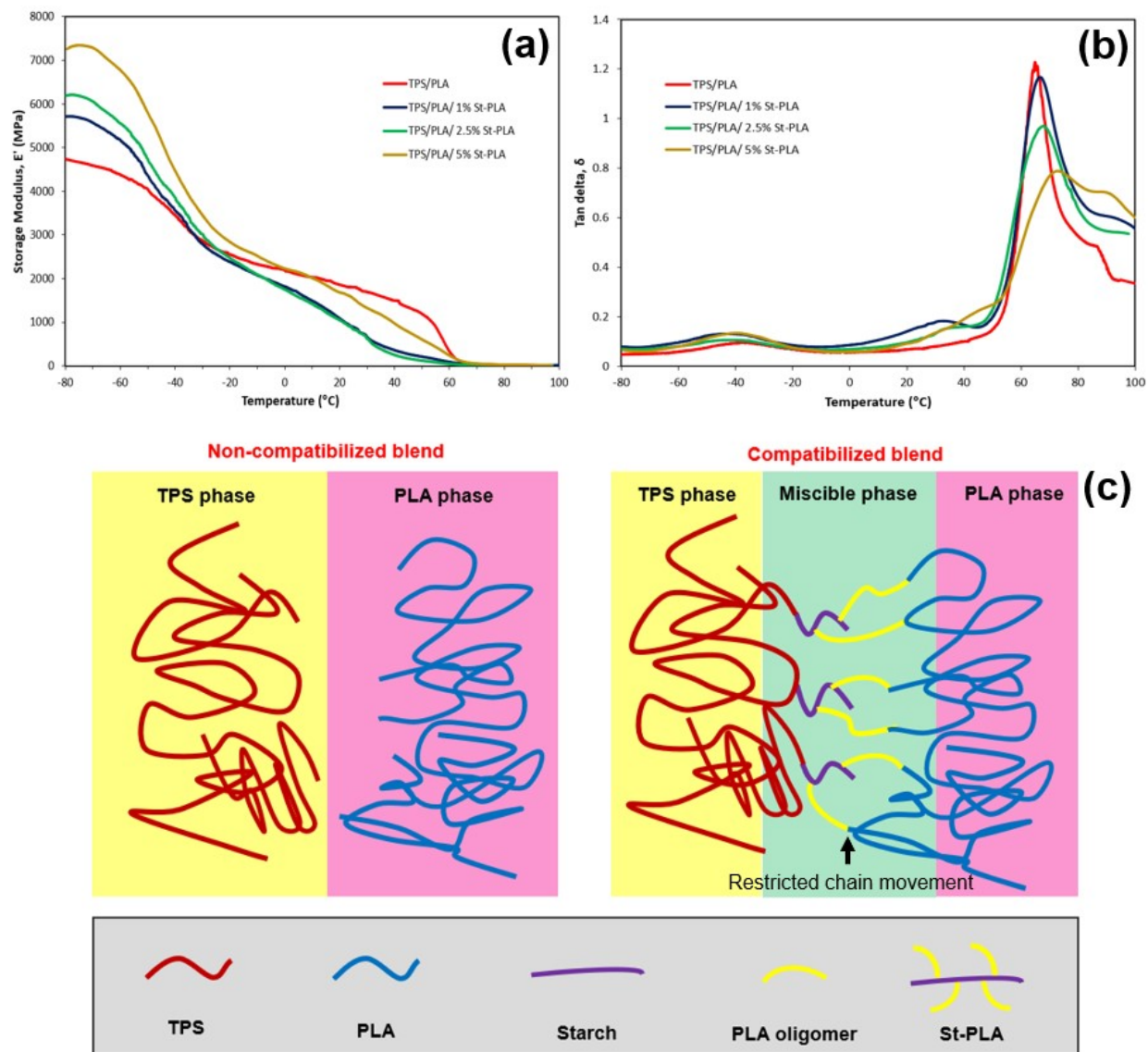


**Figure S1.** DMA results showing (a) Storage modulus, and (b) tan delta of non-compatible and compatibilized TPS/PLA blends; (c) Illustration showing the compatibilization effects of St-PLA on phase miscibility and chain mobility of TPS/PLA blends

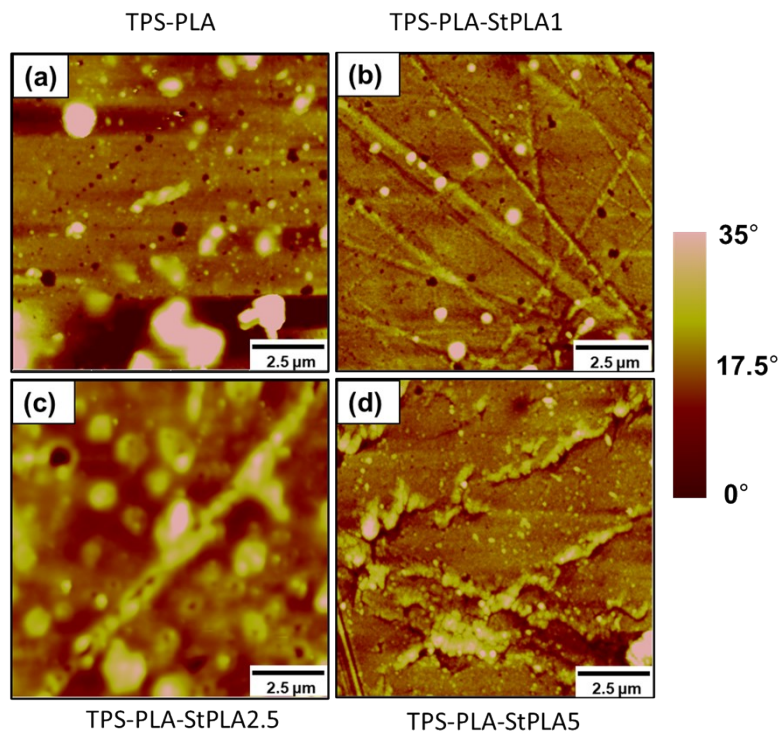


**Figure S2.** AFM images of TPS/PLA blends with and without St-PLA compatibilizer

## References

1. B.M. Trinh, E.O. Ogunsona, T.H. Mekonnen, Thin-structured and compostable wood fiber-polymer biocomposites: Fabrication and performance evaluation, *Compos. Part A Appl. Sci. Manuf.* 140 (2021) 106150. <https://doi.org/10.1016/j.compositesa.2020.106150>.
2. S. Cai, C. Zeng, N. Zhang, J. Li, M. Meyer, R.H. Fink, D. Shi, J. Ren, Enhanced mechanical properties of PLA/PLAE blends via well-dispersed and compatilized nanostructures in the matrix, *RSC Adv.* 6 (2016) 25531–25540. <https://doi.org/10.1039/C6RA01367H>.